IRASA International Scientific Conference
SCIENCE, EDUCATION, TECHNOLOGY AND INNOVATION
SETI VI 2024
Book of Proceedings

DOI: `https://doi.org/10.62982/seti06.mipr.09

EXPERIMENTAL INVESTIGATION OF THE TERNARY – NICKEL BASED ALLOYS

Milena Zečević[36], *Duško Minić*[37], *Aleksandar Đorđević*[338]

Abstract

This study presents the results of experimental test of the microstructure, hardness and electrical properties of the ternary Ni-based alloys. In the experimental part of the study, alloys of selected compositions were prepared and then examined using scanning electron microscopy (SEM) and energy dispersive spectrometry (EDS), X-ray powder diffraction (XRD), hardness measurements by Brinell method and electrical conductivity measurements. Extrapolated is isothermal section at 25 °C using optimized thermodynamic parameters from literature. The equilibrium phase diagram of the ternary systems was calculated using the Calphad method and the corresponding thermodynamic program (Pandat ver. 8.1). The results include calculated characteristic isothermal sections, structural characteristics, phase composition, mechanical properties and electrical conductivity for investigation ternary systems. Experimentally obtained results were compared with the results of thermodynamic calculation of phase diagrams. Good overall agreement between experimental and calculated values was obtained. Hardness and electrical conductivity properties were predicted in the whole composition range by using appropriated mathematical model.

Key words: *Microstructure, hardness properties, electrical conductivity, mathematical model.*

Introduction

Nickel and nickel-based alloys are widely used in various industries such as chemical, automotive, marine etc. for making vessels, pipes, heat exchangers, pumps, impellers, valves, and other type of equipment [1]. For example, nickel with copper has a variety of applications [2-4]. Especially, Cu-Ni and Cu-Ni-based alloys are used for making parts in the electronics industry [5-8] e.g. for alkaline batteries, gas engines and

[36] Associate Professor Milena Zečević, PhD, Academician of IRASA, University of Priština, Faculty of Technical Science, Kos. Mitrovica, Republic of Serbia, milena.premovic@gmail.com
[37] Full Professor Duško Minić, PhD, Academician of IRASA, University of Priština, Faculty of Technical Science, Kos. Mitrovica, Republic of Serbia, dminic65@mts.rs
[38] Assistant Professor Aleksandar Đorđević, PhD, Academician of IRASA, University of Priština, Faculty of Technical Science, Kos. Mitrovica, Republic of Serbia, coadjordjevic90@gmail.com

turbines [9], optical mirrors [10, 11], equipment for food, chemical and petrochemical industries, as well as for galvanic coating of steel objects. The most commonly used Ni-Cu alloy is Monel [12-14], which is primarily composed of nickel (up to 67%) and copper, with small amounts of iron, manganese, carbon, and silicon.
Wide application of nickel and nickel based alloys is due to the good properties such as good corrosion resistance [15–18], mechanical [19–21], magnetic [22, 23] and optical properties [24]. Due to the fact of wide nickel alloys application there is still a gap in studed Ni based alloys. In this studi research work is related to the Bi-Ni-Pb, Bi-In-Ni and Cu-In-Ni systems. The research work is based on the extrapolation of isothermal section at 300 ºC which are checked and confirmed by EDS and XRD analysis. Selected alloys from ternary systems are used for mechanical and electrical conductivity tests.

Experimental procedure

Studied alloy samples were prepared by melting of Bi (99.99 at. %), Ni (99.99 at. %), Pb (99.99 at. %), In (99.99 at.%) and Cu (99.99 at.%) shots in alumina crucibles under argon atmosphere using induction furnace. The alloys were melted and cooled repeatedly to ensure compositional homogeneity. Masses of the samples were about 3 g. The total mass losses of the prepared samples after induction melting were less than 0.5%. After melting, the samples used for SEM–EDS and XRD investigations, were placed into quartz glass ampoules, sealed under vacuum, equilibrated at 300 ºC for two weeks and then quenched into ice water. The equilibrium compositions of phases were determined by using JEOL JSM- 6460 scanning electron microscope with energy dispersive spectrometer, EDS (Oxford Instruments). All SEM images of the microstructures were taken on the polished surfaces of the studied alloy samples in backscattered electron mode. Powder XRD data for phase identification were recorded on a D8 ADVANCED and D2 Phaser. D8 ADVANCED (Bruker) powder diffractometer equipped with a dynamic scintillation detector and ceramic X-ray Cu tube (KFL-Cu-2K) in the range 10º–120º 2θ with a step size of 0.02º. D2 PHASER powder diffractometer equipped with a dynamic scintillation detector and ceramic X-ray Cu tube (KFLCu-2K) in a 2θ range of 5 to 75º with a step size of 0.02º. The patterns were analyzed using the Topas 4.2 software and ICDD databases PDF2 (2013). Electrical conductivity measurements were carried out by using Foerster SIGMATEST 2.069 instrument. At last step on same samples, the hardness of the samples was determined by using a Brinell hardness tester INNOVATEST, model Nexus 3001.

Results and Discussion

Phase equilibria in the Cu–Ni binary system have been studied extensively over the years [25–28]. Solidus and liquidus temperatures of this system were experimentally determined by Feest and Doherty [29], Schürmann and Schulz [30] and Predel and Mohs [31]. Moreover, some earlier modeling of the solid–liquid equilibria has been carried out by different authors [32–38]. On the basis of thermodynamic calculations, Meijering [39] and Elford et al. [40] have proposed the existence of a miscibility gap in

the solid state at low temperatures. In addition, a demixing in the solid solutions has also been suggested by Hong et al. [41], Larrain [42] and Notin et al. [43], whereas Sachtler et al. [44] have experimentally determined a demixing of solid solutions in thin films. Several studies on the thermodynamic activities of liquid alloys [45–48] and enthalpies of mixing of liquid Cu–Ni alloys [49–51] can be found in literature. Evaluation of thermodynamic data and phase equilibria by Jansson [35] and en Mey [33] has shown that the values obtained by Tomiska and Neckel [26] are in very close agreement with the total set of thermodynamic data for this system. Thermodynamic activities for solid Cu–Ni alloys were reported by Moser et al. [51], Notin et al. [43], Katayama et al. [52], Kontopoulos [53] and Vrestal and Stransky [54]. Enthalpies of formation of the solid alloys were determined by Kubaschewski and Spencer [26] Jansson [35] and an Mey [33], while excess entropies of formation were calculated by an Mey [33]. The thermodynamic parameters for the Cu–Ni binary system used in the current study were taken from an Mey [33]. The calculated phase diagram of Cu-Ni system is presented in Fig. 1.

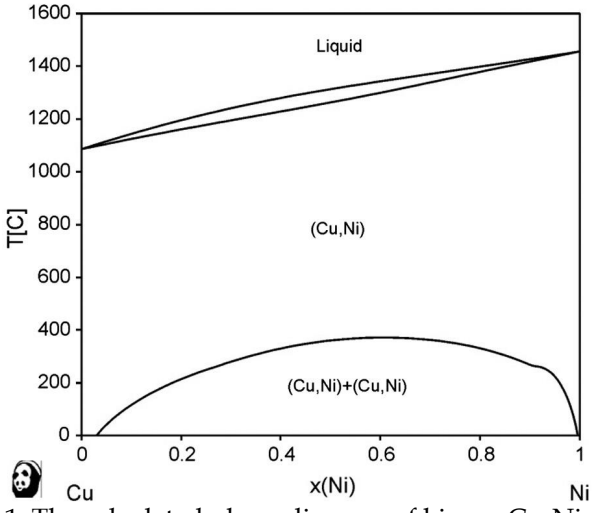

Figure 1: The calculated phase diagram of binary Cu-Ni system.

In the first study Ni-Cu alloys were alloyed with In. The calculated isothermal section of the Cu-In-Ni ternary system at 300 ^{o}C is presented in Fig. 2. The alloy samples selected for experimental investigation are also marked in Fig. 2. Compositions of the selected alloy samples lie along three vertical sections red squares Cu-In0.5Ni0.5, violet squares In-Cu0.8Ni0.2 and blue squares x(In) = 0.4 of the studied ternary system. The all selected samples marked in Fig. 2 were investigated using the same experimental techniques. Out of all predicted regions from the isothermal section at 300 ^{o}C, seven regions were selected and investigated. Six of the investigated regions are three-phase regions and the remaining one is a two-phase region.

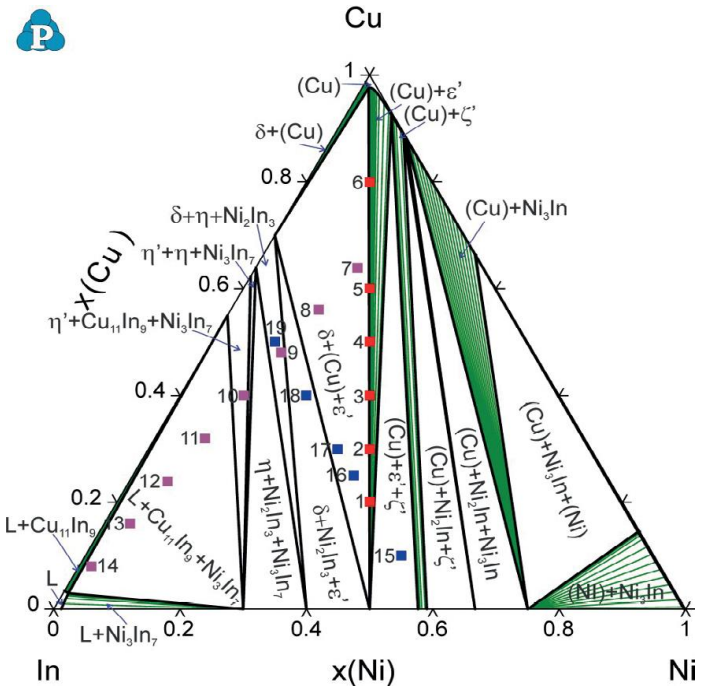

Fig. 2: Isothermal section of Cu-In-Ni system at 300 ºC.

According to the thermodynamic calculations, (see Fig. 2) samples from number 1 to 6 belong to the two-phase region (Cu)+ ε'(NiIn). The obtained experimental results of these six alloy samples confirm the existence of this two-phase region. In all cases, the solubility of copper in intermetallic phase ε'(NiIn) was found to be less than 1 at. % and thus it was negligible. Also in the case of the solid solution (Cu), the detected solubility of In was negligible. The other obtained results related to the identified phases were found to be the same as predicted so the existence of all predicted regions was confirmed. Moreover, the subsequent XRD analysis has also confirmed the presence of the same phases as were predicted by thermodynamic calculations and determined by EDS analysis. Figure 3 shows microstructures of the six alloy samples selected out of nineteen studied alloys.

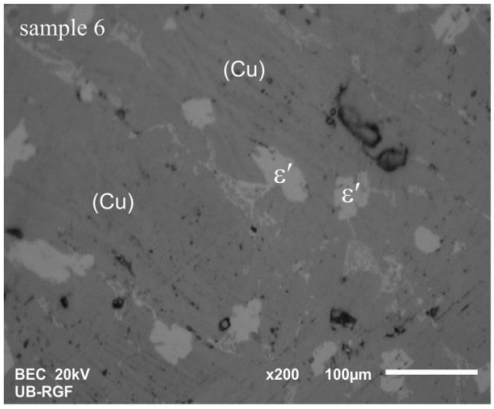

(a) sample 6

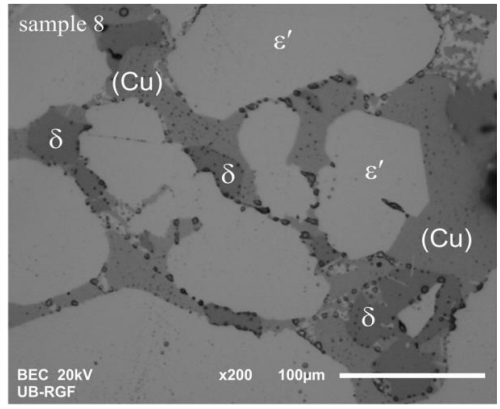

(b) sample 8

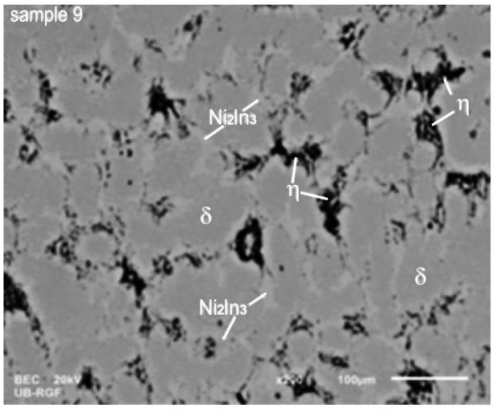

(c) sample 9

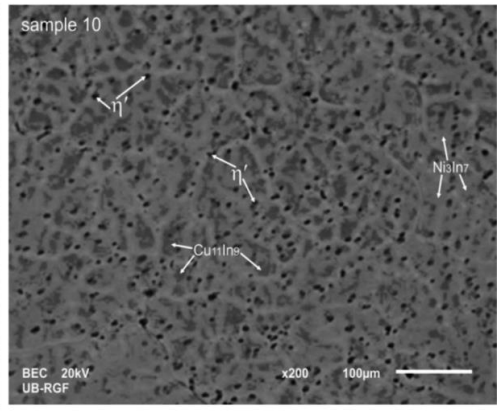

(d) sample 10

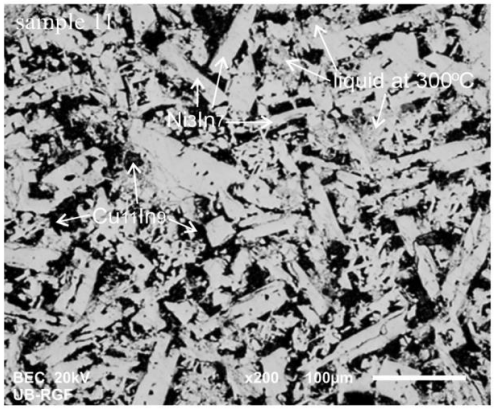

(e) sample 11

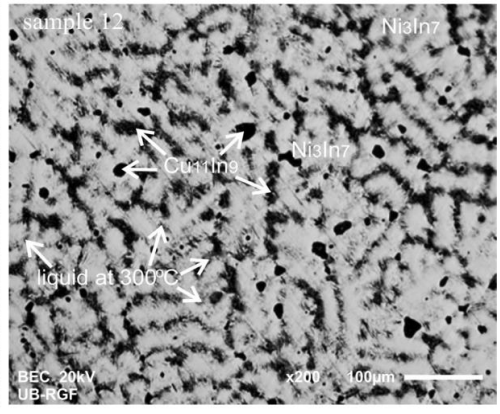

(f) sample 12

Figure 3: Microstructures of the alloys analyzed using SEM-EDS technique: a) sample 6, b) sample 8, c) sample 9, d) sample 10, e) sample 11 and f) sample 12.

Sample 6 belongs to the two-phase region while the rest samples 8, 9, 10, 11 and 12 are from three-phase regions. The phases identified using the results of energy dispersive spectrometry (EDS) are marked on the presented microstructures. In microstructure of sample 6, two phases are visible, solid solution (Cu) which is a dominant phase and binary intermetallic compound ε'(NiIn). Three phase region δ(Cu_7In_3)+(Cu)+ε'(NiIn) is visible at the microstructure of sample 8. The alloy samples 9 and 10 (Fig.3c and Fig.3d) also belong to three-phase regions. As can be seen from Fig.3c the δ phase is the most dominant phase within the microstructure of sample 9 where as Ni_2In_3 intermetallic compound appears as light phase situated at its grain boundaries. The alloy sample 10 (Fig.3d) seems to have more fine-grained microstructure compared to the rest of the studied alloy samples. In its microstructure (Fig.3d) η' phase can be observed as a small, black and round phase evenly distributed throughout the microstructure of the alloy. The samples 11 and 12 belong to the three-phase region in which liquid phase L is present (L+Ni_3In_7+$Cu_{11}In_9$). It can be observed in Fig.3e and Fig.3f as the dark phase trapped between intermetallic compounds. The intermetallic compound $Cu_{11}In_9$ appears as the darkest phase in the microstructures of the alloy samples 11 and 12 while the Ni3In7 intermetallic compound is the most abundant phase.

Two XRD patterns with identified phases, one for the sample 1 and the other for the sample 15 are shown in Figure 4, as an illustration.

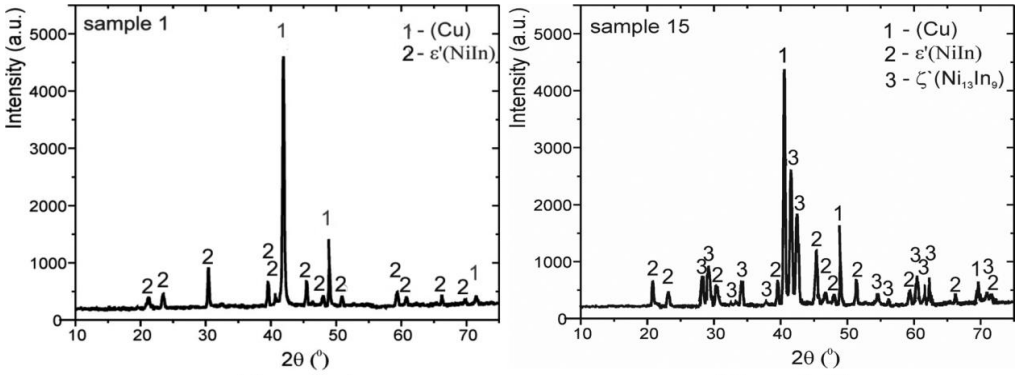

Figure 4: XRD patterns of the studied alloys: a) sample 1 and b) sample 15.

The hardness of the alloys of the Cu-In-Ni ternary system was determined using Brinell method. Measured values of the Brinell hardness of the studied alloy samples, three binary alloys (B1, B2, and B3) and literature values for pure elements [55] are graphically presented on figure 5. The experimentally obtained results clearly point out that Cu rich ternary alloys have a higher value of hardness. From all ternary alloys, alloy $Cu_{80}In_{10}Ni_{10}$ have the highest hardness. Experimentally determined value is 423.4 MN/m². The ternary alloy $Cu_{80}In_{10}Ni_{10}$ consists of the two-phase solid solution (Cu) and intermetallic compound ε'(NiIn). Since the solid solution (Cu) is in majority

and hardest phase in this system it is expected that this will influence on hardness which is experimentally determined and results that alloys rich with (Cu) phase have the highest hardness.

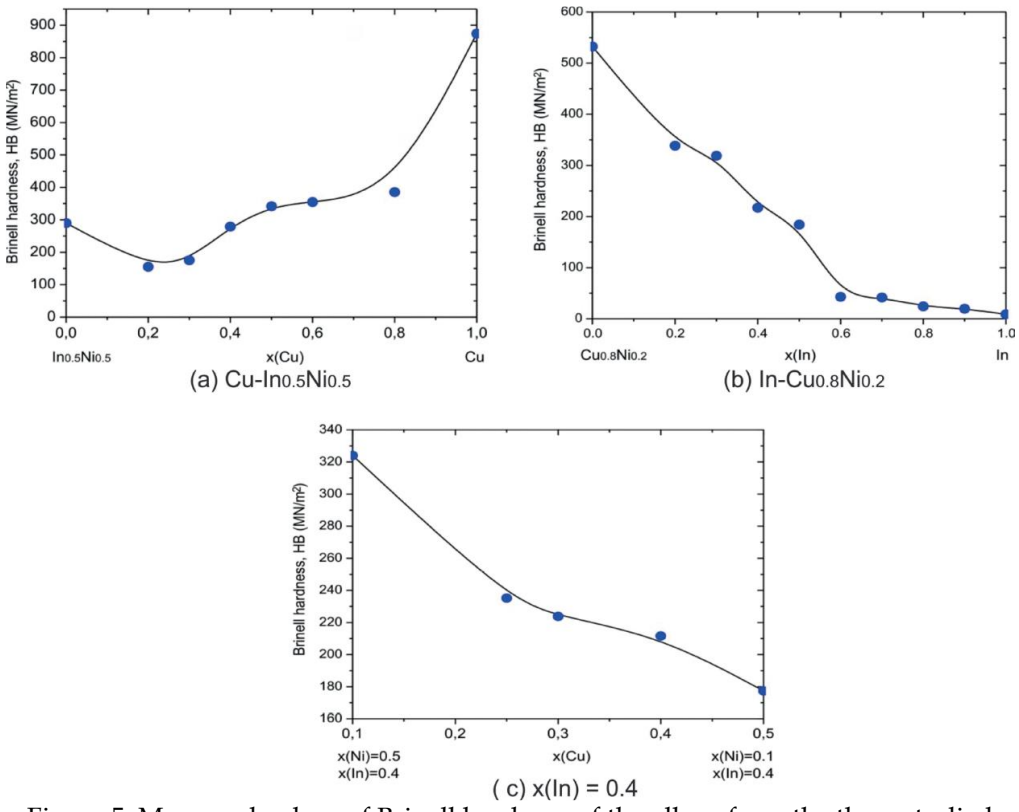

Figure 5: Measured values of Brinell hardness of the alloys from the three studied vertical sections: a) Cu-In0.5Ni0.5, b) In-Cu0.8Ni0.2 and c) x(In)=0.4.

Graphical presentation of the correlation between electrical conductivity and mole fraction of components for the all investigated samples is shown in Figure 6. The presented experimental results show that $Cu_{60}In_{20}Ni_{20}$ and $Cu_{80}In_{10}Ni_{10}$ ternary alloys have the highest electrical conductivity of the all studied ternary alloys.

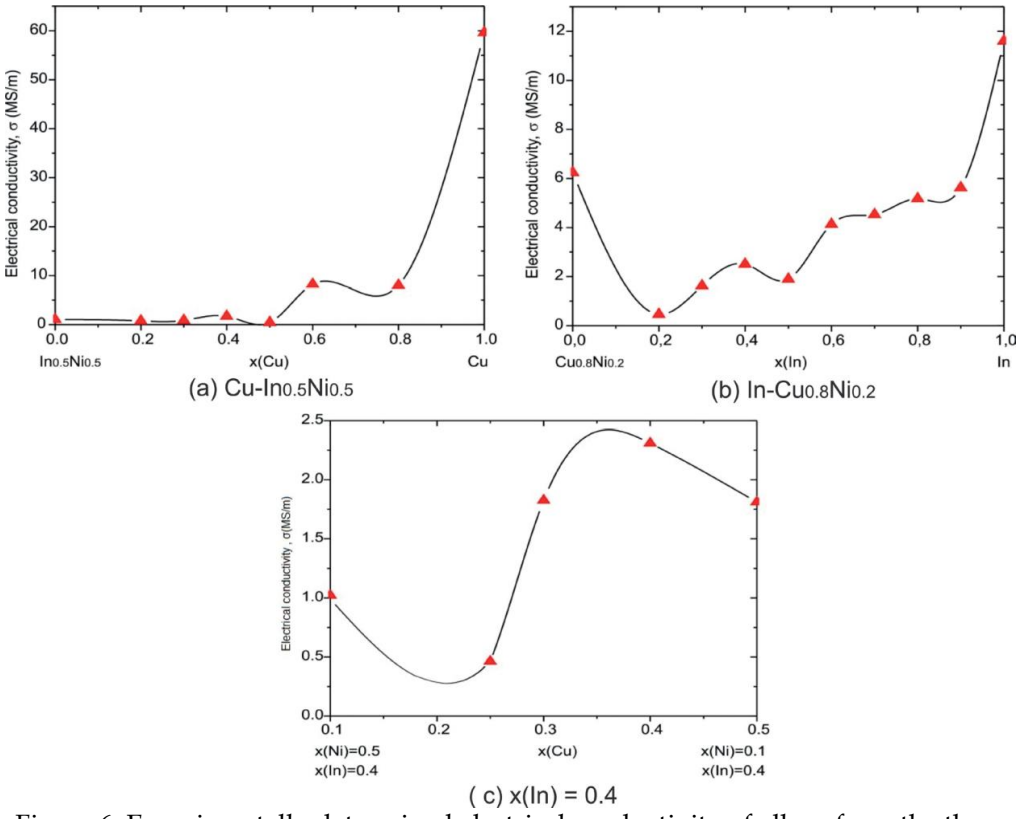

Figure 6: Experimentally determined electrical conductivity of alloys from the three studied vertical sections: a) Cu-In0.5Ni0.5, b) In-Cu0.8Ni0.2, c) x(In)=0.4.

In next study Ni were alloyed with In and Bi. The calculated isothermal section of the ternary Bi–In–Ni system at 300 ºC is presented in Fig. 7. In total, four alloy samples were analyzed using SEM–EDS method and five using XRD method. Compositions of the studied alloy samples are marked in Fig. 7, along with the predicted phases. The obtained SEM images of the microstructures of the studied alloy samples (marked in Fig. 7) are presented in Fig. 8. The presented microstructures (Fig. 8) depict presence of phases predicted by the calculations (Fig. 7).

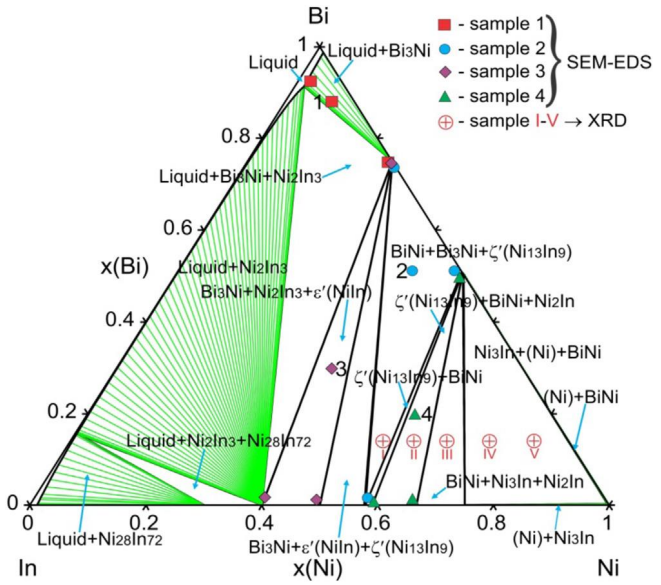

Figure 7: Calculated isothermal section of the ternary Bi–In–Ni system at 300 ºC and experimentaly determined phase compositions.

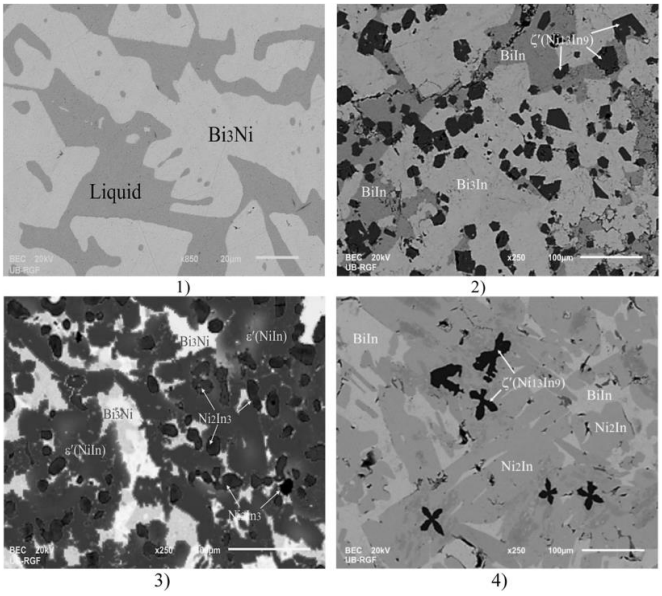

Figure 8: SEM micrographs of the samples: 1) (Bi88.3In2.8Ni8.7), 2) (Bi50.2In10.4Ni39.4), 3) (Bi30.5In32.2Ni37.3) and 4) (Bi20.4In24.8Ni54.8) (at.%).

The obtained diffractograms of the studied $Bi_{14}In_{32}Ni_{54}$, $Bi_{10.3}In_{24.2}Ni_{65.5}$ and $Bi_{60.5}In_{29.8}Ni_{9.7}$ alloy samples with marked identified phases Bi_3Ni, BiNi and $Ni_{13}In_9$ are presented in Fig. 9.

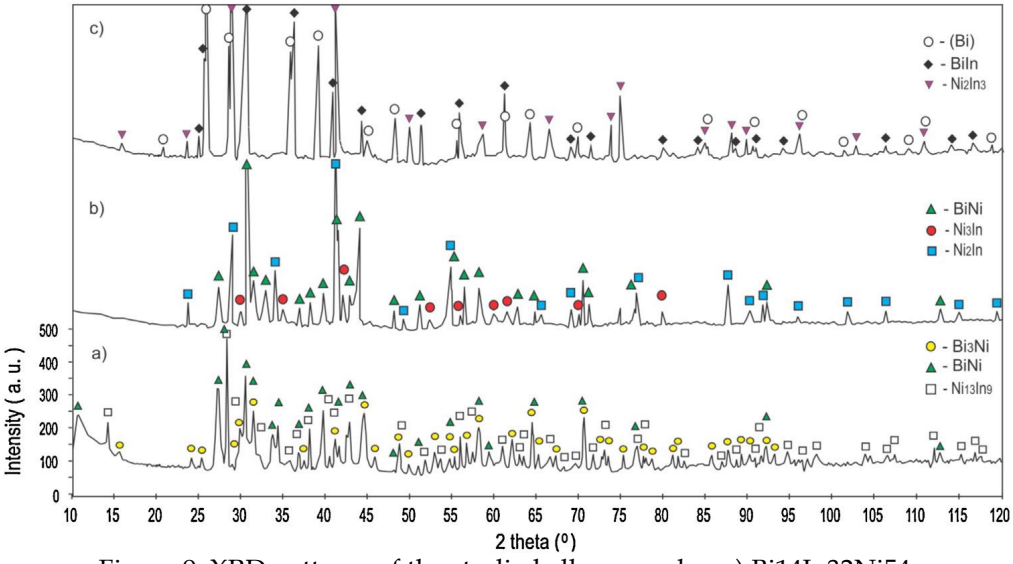

Figure 9. XRD patterns of the studied alloy samples: a) Bi14In32Ni54, b) Bi10.3In24.2Ni65.5 and c) Bi60.5In29.8Ni9.7 (at.%).

As the next example, Ni is alloyed with Bi and Pb. Figure 10 presents the calculated isothermal section at 300 °C compared with the obtained experimental data.

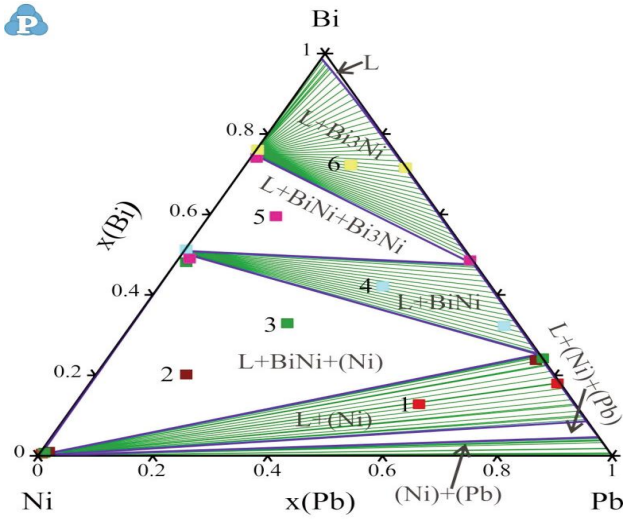

Figure 10: Calculated isothermal section of the ternary Bi–Ni-Pb system at 300 °C compared with the experimental data.

The calculated isothermal section at 300 °C was found to consist of eight different phase regions. One is single-phase region where Liquid, L phase exist, four are two phase regions (Ni)+(Pb), L+(Ni), L+BiNi, and L+Bi_3Ni, and remaining three are threephase regions L+(Ni)+(Pb), L+BiNi+(Ni), and L+BiNi+Bi_3Ni. Five out of the eight phase regions predicted by thermodynamic calculations were experimentally detected, the three two-phase regions and the two three-phase regions. The existence of the two-phase regions L+(Ni), L+BiNi, and L+Bi_3Ni was confirmed within the alloy samples 1, 4 and 6, respectively. Within the samples 2 and 3, presence of the three-phase region L+BiNi+(Ni) was confirmed, and within the sample 5 presence of the another threephase region L+BiNi+Bi_3Ni was confirmed. The determined compositions of the studied alloy samples and each of the identified phases are marked in Figure 10 (the same color of squares was used for marking of the sample compositions and compositions of the associated phases). From Fig. 10 it can be seen that the experimentally determined phase compositions support the results of thermodynamic calculations rather well.
Fig. 11 a) presents microstructure of the sample 3, in which three phases are visible. The identified phases are marked with their corresponding names. The darkest phase in Fig. 11 a) is a (Ni) solid solution, the grey phase is a binary intermetallic compound BiNi, and the light phase is a Liquid, L phase. Within the microstructure of the sample 4, presented in Figure 11 b), two phases in equilibrium can be observed, the grey phase which is a BiNi intermetallic compound and the light phase which represents a Liquid, L phase.

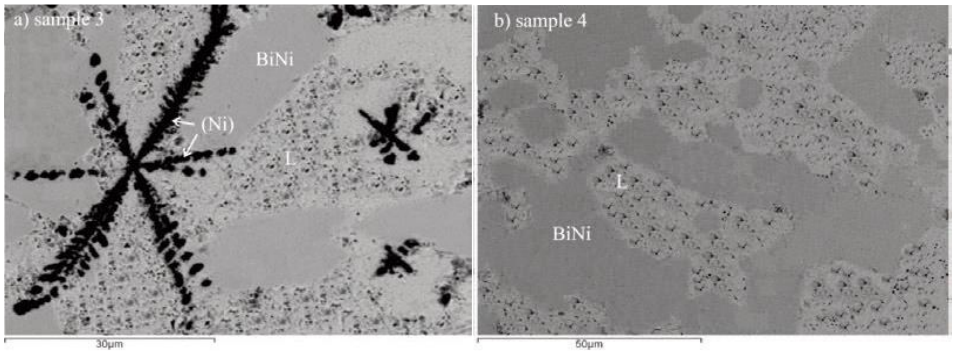

Figure 11 : SEM micrographs of the selected alloy samples annealed at 300 °C for five weeks: a) sample 3 and b) sample 4.

Figure 12 presents XRD patterns of sample 6, with marked peaks of Bi_3Ni phase.

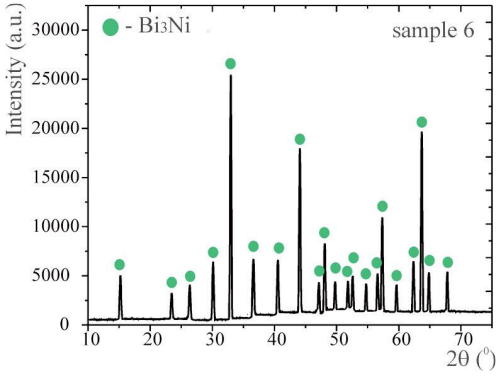

Figure 12: XRD pattern for the alloy sample 6.

Conclusions

Three different ternary systems based on Ni were tested. Tested alloys were from isothermal section at 300 ºC. All alloys were tested with SEM-EDS and XRD. A close agreement between the experimental results and the calculated isothermal section was obtained. The tested ternary systems and the extrapolated isothermal sections are important for the future development of Ni-based alloys.

Acknowledgements

This work has been supported by the Ministry of Education, Science and Technological Development of the Republic of Serbia, project No. OI172037.

References

[1] Chen J, Wang J, Yan F, Zhang Q, Li Q. Effect of applied potential on the tribocorrosion behaviors of Monel K500 alloy in artificial seawater. *Tribology International*. 2015; 81:1-8.
[2] Carrera AJ, Cangiano MA, Ojeda MW, Ruiz MC. Characterization of Cu-Ni nanostructured alloys obtained by a chemical route. Influence of the complexing agent content in the starting solution. *Materials Characterization*. 2015; 101:40-48.
[3] Cui S, Zhang L, Du Y, Zhao D, Xu H, Zhang W, et al. Assessment of atomic mobilities in fcc Cu-Ni-Zn alloys. *Calphad*. 2011; 35(2):231-241.
[4] Xu X, Zhu N, Zheng W, Lu XG. Experimental and computational study of interdiffusion for fcc Ni-Cu-Cr alloys. *Calphad*. 2016; 52:78-87.
[5] Semboshi S, Sato S, Iwase A, Takasugi T. Discontinuous precipitates in age-hardening Cu-Ni-Si alloys. *Materials Characterization*. 2016; 115:39-45.
[6] Lei J, Xie H, Tao S, Zhang R, Lu Z. Microstructure and Selection of Grain Boundary Phase of Cu-Ni-Si Ternary Alloys. *Rare Metal Materials and Engineering*. 2015; 44(12):3050-3054.

[7] Samal CP, Parihar JS, Chaira D. The effect of milling and sintering techniques on mechanical properties of Cu-graphite metal matrix composite prepared by powder metallurgy route. *Journal of Alloys and Compounds*. 2013; 569:95-101.
[8] Masrour R, Hamedoun M, Benyoussef A, Hlil EK. Magnetic properties of mixed Ni-Cu ferrites calculated using mean field approach. *Journal of Magnetism and Magnetic Materials*. 2014; 363:1-5.
[9] Badawy WA, El-Rabiee M, Helal NH, Nady H. The role of Ni in the surface stability of Cu-Al-Ni ternary alloys in sulfatechloride solutions. *Electrochimica Acta*. 2012; 71:50-57.
[10] Calleja P, Esteve J, Cojocaru P, Magagnin L, Vallés E, Gómez E. Developing plating baths for the production of reflective Ni-Cu films. *Electrochimica Acta*. 2012; 62:381-389.
[11] Nagarjuna S, Srinivas M, Sharma KK. The grain size dependence of flow stress in a Cu-26Ni-17Zn alloy. *Acta Materialia*. 2000; 48(8):1807-1813.
[12] Milošev I, Metikoš-Huković M. The behaviour of Cu-xNi (x = 10 to 40 wt%) alloys in alkaline solutions containing chloride ions. *Electrochimica Acta*. 1997; 42(10):1537-1548.
[13] Li B, Gu J, Wang Q, Ji C, Wang Y, Qiang J, Dong C. Cluster formula of Fe-containing Monel alloys with high corrosionresistance. *Materials Characterization*. 2012; 68:94-101.
[14] Ganley JC. High temperature and pressure alkaline electrolysis. *International Journal of Hydrogen Energy*. 2009; 34(9):3604-3611.
[15] M. Metikos-Hukovica, I. Skugorb, Z. Grubacb, R. Babic, Electrochim. *Acta 55* (2010) 3123–3129.
[16] A.A. Khadom, A.S. Yaro, Russ. *J. Phys. Chem*. A 85 (2011) 2005–2012.
[17] S. Mukherjee, A.K. Ghosh, *Mater. Sci. Eng*. A 528 (2011) 3289–3294.
[18] A.A. Khadom, A.S. Yaro, A.Y. Musa, A.B. Mohamad, A.H. Kadhum, J. Korean *Chem. Soc.* 56 (2012) 406–415.
[19] S. Bhattacharya, G.P. Dinda, A.K. Dasgupta, H. Natu, B. Dutta, J. Mazumder, *J. Alloys Comp*. 509 (2011) 6364–6373.
[20] E. Pellicer, A. Varea, S. Pane, K.M. Sivaraman, B.J. Nelson, S. Surinach, M.D. Baro, *J. Sort, Surf. Coat. Technol*. 205 (2011) 5285–5293.
[21] A. Varea, E. Pellicer, S. Pane, B.J. Nelson, S. Surinach, M.D. Baro, J. Sort, *Int. J. Electrochem. Sci.* 7 (2012) 1288–1302.
[22] I. Baskaran, T.S.N. Sankara Narayanan, A. Stephen, *Mater. Lett.* 60 (2006) 1990–1995.
[23] M. Alper, H. Kockar, M. Safak, M.C. Baykul, *J. Alloys Comp*. 453 (2008) 15–19.
[24] P. Calleja, J. Esteve, P. Cojocaru, L. Magagnin, E. Valles, E. Gomez, *Electrochim. Acta* 62 (2012) 381–389.
[25] W. Guertler, G. Tammann, *Z. Anorg. Chem* 52 (1907) 25–29.
[26] N.S. Kurnakov, S.F. Zemcznzny, Zh. Russ. *Fiz. Khim*. 39 (1907) 211.
[27] P. de Cesaris, *Gazz. Chim. Ital*. 43 (1913) 365–379.
[28] M. Hansen, K. Anderko, *Constitution of Binary Alloys*, McGraw-Hill Book Comp., New York, 1958.

[29] A.E. Feest, R.D. Doherty, *J. Inst. Met*. 99 (1971) 102.
[30] E. Schürmann, E. Schulz, *Z. Metallkd*. 62 (1971) 758.
[31] B. Predel, R. Mohs, *Arch. Eisenhüttenwes*. 42 (1971) 575–579.
[32] O. Kubaschewski, P.J. Spencer, *J. Less-Common Met*. 114 (1985) 43–47.
[33] S. an Mey, Z. *Metallkd*. 78 (1987) 502.
[34] F. Lihl, H. Ebel, A. Reichl, A. Kaminitschek, Z. *Metallkd*. 59 (1968) 735.
[35] G. Faninger, Z. *Metallkd*. 62 (1971) 152.
[36] A. Jansson, Materials Research Center, The Royal Inst. of Technology, Stockholm, 1987.
[37] J. Tomiska, A. Neckel, *Ber. Bunsenges. Phys. Chem*. 88 (1984) 551–557.
[38] R.C. Sharma, *Trans. Indian Inst. Met*. 35 (1982) 372–375.
[39] J.L. Meijering, *Acta Metall*. 5 (1957) 257–264.
[40] L. Elford, F. Müller, O. Kubaschewski, *Ber. Bunsenges. Phys. Chem*. 73 (1969) 601–605.
[41] S.I. Hong, I.S. Choi, S.W. Nam, *J. Mater. Sci*. 19 (5) (1984) 1672–1679.
[42] J.M. Larrain, *Can. Metall. Q* 18 (1979) 401–406.
[43] M. Notin, G. Lefebvre, J. Hertz, *J. Solid State Chem*. 28 (1979) 109–120.
[44] W.M.H. Sachtler, G.J.H. Dorgelo, J. *Catalysis* 4 (1965) 654–664.
[45] C.W. Schultz, G.R. Zellars, S.L. Payne, E.F. Foerster, U.S. Bureau of Mines, Rept. Investig. No. 6410 (1964).
[46] R. Hultgren, P.D. Desai, D.T. Hawkins, M. Gleiser, K.K. Kelley, Selected Values of Thermodynamic Properties of Binary Alloys, *Amer. Soc. for Metals*, Metals Park (Ohio), 1973.
[47] A.D. Kulkarni, R.E. Johnson, *Metall. Trans*. 4 (1973) 1723.
[48] Yu.T. Melnikov, V.E. Novoselov, *Russ. J. Phys. Chem*. 50 (1976) 1416.
[49] J. Tomiska, A. Neckel, Int. J. Mass-Spectrom. *Ion Phys*. 47 (1982) 223–226.
[50] Y. Yozaki, Y. Iguchi, S. Ban-Ya, T. Fuwa, in: *Proc. Int. Symp. of Chem. Metallurgy of Iron and Steel*, 1971, pp. 130.
[51] M.J. Pool, I. Arpshofen, B. Predel, E. Schultheiss, Z. *Metallkd*. 70 (1979) 656.
[52] Z. Moser, W. Zakulski, P. Spencer, K. Hark, *Calphad* 9 (3) (1985) 257–269.
[53] J. Katayama, H. Shimateni, Z. Kozuka, *Nippon Kinzoku Gakkaishi* 37 (1973) 509.
[54] A. Kontopoulos, *Trans. Inst. Min. Metall*. C 87 (1978) 1–5.
[55] Webelements. Hardness - Brinell. Available from: <http://www.webelements